High performance shear thickening fluid based on calcinated colloidal silica microspheres

2015 Smart Mater. Struct. 24 085033

(http://iopscience.iop.org/0964-1726/24/8/085033)

IOP Publishing Smart Materials and Structures
Smart Mater. Struct. 24 (2015) 085033 (8pp) doi:10.1088/0964-1726/24/8/085033

High performance shear thickening fluid based on calcinated colloidal silica microspheres

Sheng-Biao Zheng[1,3], Shou-Hu Xuan[2], Wan-Quan Jiang[1] and Xing-Long Gong[2]

[1] Department of Chemistry, University of Science and Technology of China, Hefei 230026, People's Republic of China
[2] CAS Key Laboratory of Mechanical Behavior and Design of Materials, Department of Modern Mechanics, University of Science and Technology of China, Hefei 230027, People's Republic of China
[3] College of Chemistry and Materials Engineering, Anhui Science and Technology University, Fengyang 233100, People's Republic of China

E-mail: jiangwq@ustc.edu.cn and gongxl@ustc.edu.cn

Received 23 April 2015, revised 28 May 2015
Accepted for publication 4 June 2015
Published 23 July 2015

Abstract

Here, a novel method to prepare high performance shear thickening fluids (STFs) by dispersing calcinated silica microspheres into ethylene glycol is reported. The silica particles were prepared by hydrolyzing tetraethylorthosilicate (TEOS), and then they were treated under high temperature to remove the physically adsorbed water and the -OH groups on the surfaces. The influence of the temperature on the rheological properties of the final STFs was investigated and the STF prepared under the optimum temperature exhibited the best ST effects. A possible mechanism was proposed and it was found that a proper solvation layer adsorbed on the silica surface resulted in lower critical shear rate and higher shear thickening viscosity.

Keywords: shear thickening, silica microspheres, suspensions, rheology

(Some figures may appear in colour only in the online journal)

1. Introduction

Shear thickening fluid (STF) is a type of non-Newton fluids whose viscosity usually presented a sharp increase when it encountered an unexpected impact or shear. Due to this unique shear-thickening (ST) property, it has been widely applied in liquid coupling, shock absorbers, damping devices, control devices, rotary speed limiters, and body armor [1–6]. The STF was prepared by dispersing solid particles into the carrier solvent. It was proposed that these solid particles formed ordered two-dimensional structures in the suspension. If the external shear stress reached a critical level, ordered layers broke and jammed, causing the viscosity to rise [7–9]. Moreover, the reversible ST in concentrated dispersions was ascribed to the formation of jamming clusters arising from hydrodynamic lubrication forces between particles [10–14].

The solid particles played a critical role in determining the rheological properties of the STF. Various colloidal particles, such as clay, calcium carbonate, silica, titania, starch particles, and polymer spheres, were important starting materials for preparing the high performance STFs [1–12, 14–17]. The intrinsic characteristics of the dispersing particles showed unique influence on the rheological behavior of the relative STFs. In comparison to the hard spheres, the soft spheres lead to a smaller yield strain; thus, a larger shear rate was needed for the ST phenomenon [18]. With increasing the crosslinking density of the polymer spheres, the ST effects improve. Besides the hardness, the interparticle forces also had a strong high influence on the ST behavior [19–22]. By increasing the repulsive forces between the dispersed particles, the starting shear rate for the ST increased. As the suspension presented ST behavior at volume fractions of particles near the maximum packing, the critical shear rate decreased with increasing volume fraction. Because the interparticle forces were highly dependent on the surface state of the solid particles, the study of the surface characteristics

was proven to be an essential part to investigate the ST mechanism [23, 24]. Several methods such as tuning the pH, ionic strength, and surface charge have been developed to improve the mechanical properties of the STFs [25–29]. It was found that the ST effects were not only dependent on the hydrodynamic interactions, but also dependent on the surface forces. Therefore, the optimum ST property should be obtained by controlling the surface characteristics of the solid particles.

Monodispersed silica microspheres based STFs were favorable because of their easy preparation and excellent mechanical properties. Various studies have been conducted on silica based STFs and their ST effects were controllable by altering the concentration, solvent, and additives [30–33]. It was reported that the silanol groups on the surface of the particles could lead to short-range electrostatic interactions, which would exhibit intensive influence on the ST effects. Moreover, the calcination can eliminate not only the physically absorbed water, but also decrease the –OH groups on the surface of the silica particles [23, 34–37]. To this end, the investigation of the heating treatment on the ST behavior for the silica particles based STF thereof is meaningful.

In this work, high performance STFs were prepared by using the calcinated silica particles as the dispersing phase. The influence of the heating temperature on the rheological properties of the STF was investigated and the optimum treating parameter was obtained. The inner structures and surface states of the calcinated silica microspheres were studied using Fourier-transform infrared spectroscopy (FT-IR), a scanning electron microscope (SEM), transmission electron microscope (TEM) and X-ray photoelectron spectroscopy (XPS) analysis. Finally, a possible mechanism for the improving ST effect was proposed. These results supplied valuable information for understanding the structural-dependent rheological properties in the concentration suspension.

2. Experimental section

The materials used in this study included tetraethylorthosilicate (TEOS, CP), ethanol (AR), ammonia (AR) and ethylene glycol (EG, AR) and were all purchased from Sinopharm Chemical Reagent Co., Ltd (China). Deionized water was made in the laboratory.

2.1. Preparation of monodispersed silica microspheres

Monodispersed silica microspheres were synthesized by hydrolyzing TEOS in a water-ethanol mixture containing ammonia according to the Stöber process [38]. The synthesis was conducted in a 2000 mL three-necked flask, which was fitted with a mechanical stirrer. Then, 1140 mL ethanol, 92 mL ammonia, and 49 mL deionized water were first added to the flask and stirred for 10 min in the 35 °C water bath. Then 54 mL tetraethyl orthosilioate was slowly introduced by dripping. After stirring for 6 h, 27 mL tetraethyl orthosilioate and 25 mL distilled water were added again. Following stirring for another 8 h, the white colloidal suspension was obtained. Suspension was centrifuged and then the silica microspheres sediment was redispersed in ethanol and sonicated for 30 min The silica nanoparticles were washed three times with ethanol and three times with deionized water. At last, the silica microspheres obtained were dried in a vacuum oven at 323 K and the final obtained particles were defined as p-SiO_2.

2.2. Calcination of monodisperse silica microspheres

The silica microspheres were calcined in a muffle furnace at 473 K, 673 K, and 873 K for 6 h at a heating rate of 10 °C min^{-1}. Then the calcination-treated silica nanoparticles were obtained and defined as c-SiO_2.

2.3. Preparation of calcinated silica microspheres based STF

The c-SiO_2 microsphere powders and ethylene glycol were added into the ball mill and then ground for 24 h at room temperature to insure even dispersion of the microspheres. Here, the ball mill is better than ultrasonic dispersion, magnetic stirring dispersion, and other methods because dispersing the silica particle clusters in EG and the surface roughness of the silica microspheres were not changed during the milling treatment. The volume fraction of the silica suspensions were kept at 61.2%. The resulting dispersions were sonicated for 1 h to remove entrained air bubbles. Then, the c-SiO_2 based STF was prepared. Here, a p-SiO_2 based STF was also prepared under a similar process.

2.4. Characterization

Morphologies of p-SiO2 and c-SiO2 were characterized by SEM, (Sirion 200, FEI, America) and TEM (JEM-2100, JEOL, Japan). The thermogravimetric (TG) measurements were carried out by the thermogravimetric analyzer (TGA Q5000IR, TA, America) over the temperature range from room temperature to 1073 K at 10 K min^{-1} of the heating rate. The sample chamber was purged with dry nitrogen at 10 mL min^{-1}. FT-IR of these silica samples were characterized by FT-IR spectra, which was performed on Nicolet 8700 infrared spectrophotometer (Nicolet, USA). The surface chemistry of the p-SiO_2 and the c-SiO_2 were characterized by x-ray photoelectron spectroscopy (XPS, Thermo-VG Scientific ESCALAB 250Xi). Rheological measurements were conducted on a stress-and-strain–controlled rheometer (Anton-Paar MCR 301, Austria) with 25 mm diameter, 0.02 radian cone, and plate geometry. The small angle of the cone minimized edge failure of the sample and hence increased the limit on the highest achievable shear rate. All tests were performed in an Anton-Paar MCR 301 rheometer with a fixed gap size of 0.05 mm, due to the cone and plate geometry measurement tool, and measurement temperature was maintained at 25 °C with an automatic temperature control device.

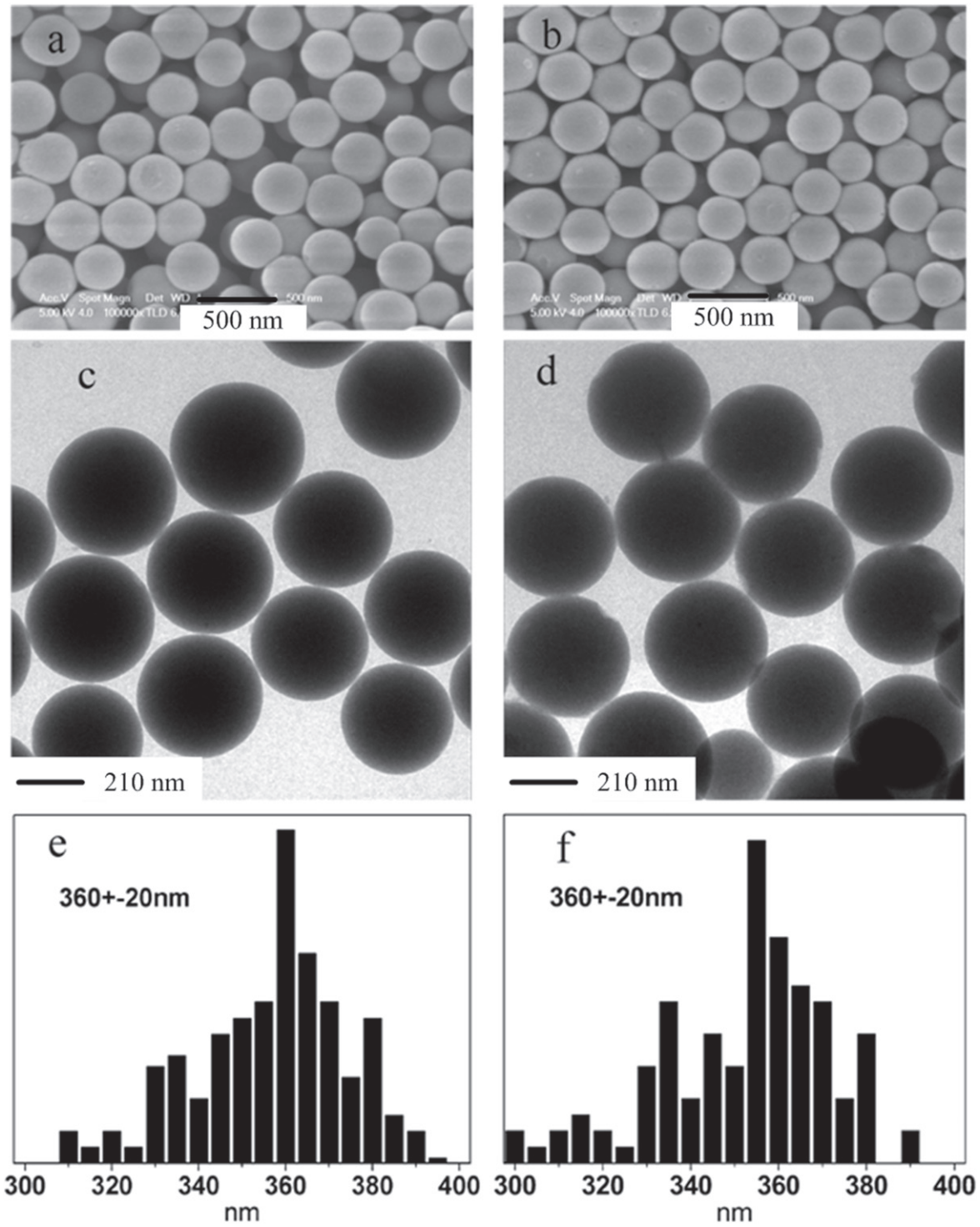

Figure 1. (a), (c) SEM and TEM images of the as-prepared p-SiO_2 and (b), (d) of c-SiO_2 (827 K) microspheres. (e), (f) are the particle size distribution histogram for p-SiO_2 and c-SiO_2 (827 K) microspheres, respectively.

3. Results and discussions

The monodispersed silica microparticles were prepared according the famous Stöber method by hydrolyzing TEOS in a water-ethanol mixture containing ammonia. Figure 1(a) presents the typical SEM image of the as-prepared p-SiO_2 microspheres, in which we can find that all the particles are spherical and the average diameter of the microspheres is about 360 ± 20 nm, according to statistics from the SEM photograph. Here, the calcination treatments show little effect on the morphology of the final particles. The c-SiO_2 possess uniform size distribution, are well dispersed on the copper grid without large aggregations, and demonstrate that no melt is occurring during calcination. To investigate the inner nanostructure of the p-SiO_2 and c-SiO_2 microspheres, the TEM was further applied to analyze the morphology.

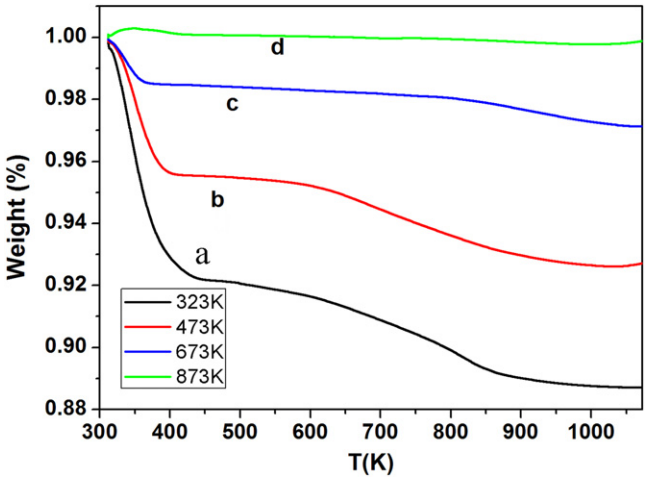

Figure 2. TG curve of the silica nanoparticles (a)–(d).

Observably, both the two particles are of same size and size distribution, which agrees well with the SEM analysis .

In this work, the c-SiO_2 microspheres were obtained by calcinating the p-SiO_2 under different temperatures. Although few changes were found in their morphologies, some differences were present in their TG curves (figure 2). For p-SiO_2, the TG curve demonstrated an 11 wt% weight loss, which must be responsible for the release of the adsorbed water and diminishing of the -OH groups on the surfaces. In contrast, the weight loss for the c-SiO_2 (473 K), c-SiO_2 (673 K), and c-SiO_2 (873 K) were 7, 2, and 0 wt%, respectively. Under higher pre-calcination temperature, more adsorbed water would be released, thus the relative c-SiO_2 possessed a smaller weight loss in the TG curve. Because of the small weight loss, no critical reduction of the diameter size was found for the silica microspheres. However, the densities of the particles were decreased after the calcination treatment. The densities of the silica particles were obtained from solution (ethanol) densitometry measurements at various solid weight fractions using a volumetric balance assuming ideal mixing. The results indicated that the p-SiO_2 particle density was $\rho = 1.78 \pm 0.01\ \mathrm{g\,cm^{-3}}$, and the calcined silica particle densities were 1.70 ± 0.01(473 K),1.66 ± 0.01 (673 K), and $1.57 \pm 0.01\ \mathrm{g\,cm^{-3}}$ (873 K), respectively. The decreased apparent density resulted from the presence of porous structure in calcined particles due to removal of the residual organic ethyoxyl from the incomplete hydrolyzing TEOS, the internal water, and the deeper silanol groups during the heating process.

The p-SiO_2 and c-SiO_2 microspheres could be dispersed into ethylene glycol to form the relative STFs. Here, to compare the calcination influence on the ST effects, all four samples were prepared by keeping the volume fraction as a constant (61.2 v/v%). Figure 3 showed the relative rheological behaviors under both steady shear and oscillatory shear. Taking the p-SiO_2 based STF as an example, its viscosity undergoes a shear-thinning and ST process. Under lower shear rate, the viscosity decreased and it was always present in the traditional STFs. As soon as the shear rates increased to $123\ \mathrm{s^{-1}}$, the viscosity sharply increased, indicating typical ST behavior. The c-SiO_2 (473 K) and c-SiO_2 (673 K) based STFs exhibited a similar phenomenon. Unfortunately, only very weak ST was found in c-SiO_2 (873 K). The shear-rate-dependent viscosity demonstrated that the calcination shows high influence on the ST effects of the STF thereof. First, with an increase of the treating temperature, the critical shear rates for the relative STFs first increased and then decreased. The critical shear rates of the suspensions were $123\ \mathrm{s^{-1}}$ (323 K), $10\ \mathrm{s^{-1}}$ (473 K), $15\ \mathrm{s^{-1}}$ (673 K), and $30\ \mathrm{s^{-1}}$ (873 K), respectively. Second, the maximum viscosity of ST dramatically increased from 40 pa·s (323 K) to 265 pa·s (473 K), decreased to 40 pa·s (673 K) and 11 pa·s (873 K) at corresponding calcined temperature. Based on the preceding results, we can conclude that the 473 K is the optimum treating condition to improve the ST effects.

Clearly, the calcination plays a critical role in determine the rheological properties of the final suspension. After calcination, the change of the silica is solely the silanol groups and physically adsorbed water on the surface of the silica particle. It was reported that the surface characteristic highly influence the ST effects through the silanol groups. The coverage of the silanol (Si-OH) groups on the fumed silica was about 2.5 silanol groups $\mathrm{nm^{-2}}$, while the value was 8.2 silanol groups $\mathrm{nm^{-2}}$ for the silica particles prepared via the Stöber process [34]. Zhuravlev reported the number of silanol groups per square nanometer is 4.6, this number was suggested as a physicochemical constant of dehydrated but fully hydroxylated amorphous silica, independent of origin and structural characteristics of the silica [35–37]. The silica surface silanol groups are the main centers of adsorption, bonding water molecules with hydrogen bonds on the silica. Therefore, the calcination affected the ST effects via changing the surface functional group on the silica microspheres.

FT-IR spectra of the raw and calcined (under various temperatures) silica nanoparticles were shown in figure 4. Both silanol groups (chemical bonded) and physically adsorbed water (hydrogen bonded) exist on the surface of silica. They are different from the bonding form; thus, water on the surface could be dehydrated with increasing calcined temperature. It was reported that the silanol groups and physically adsorbed water on surface were $8.2\ \mathrm{nm^{-2}}$ and $9.8\ \mathrm{nm^{-2}}$, respectively [34]. From the TG curve, we find the physically adsorbed water was removed mainly at 350 K. Therefore, in comparison to the p-SiO_2, the infrared absorption of H_2O at $3465\ \mathrm{cm^{-1}}$ and $1633\ \mathrm{cm^{-1}}$ for c-SiO_2 (473 K) microspheres decreased obviously, indicating that the silanol groups are hardly decreased but the physically adsorbed water was mostly removed. The removal of the physically adsorbed water facilitated the adsorbing ethylene glycol to form a solvation layer on the surface of silica nanoparticles, which gives rise to short-range, non-DLVO repulsions ('solvation forces') and stabilizes the silica particles.

The XPS is a very good technique for detecting the surface state of the particles [39, 40]. Figure 5 presents the typical XPS spectra of the silica particles treated under different calcinations temperatures, which indicates all the particles have a similar surface state. The intense peak at 285 eV,

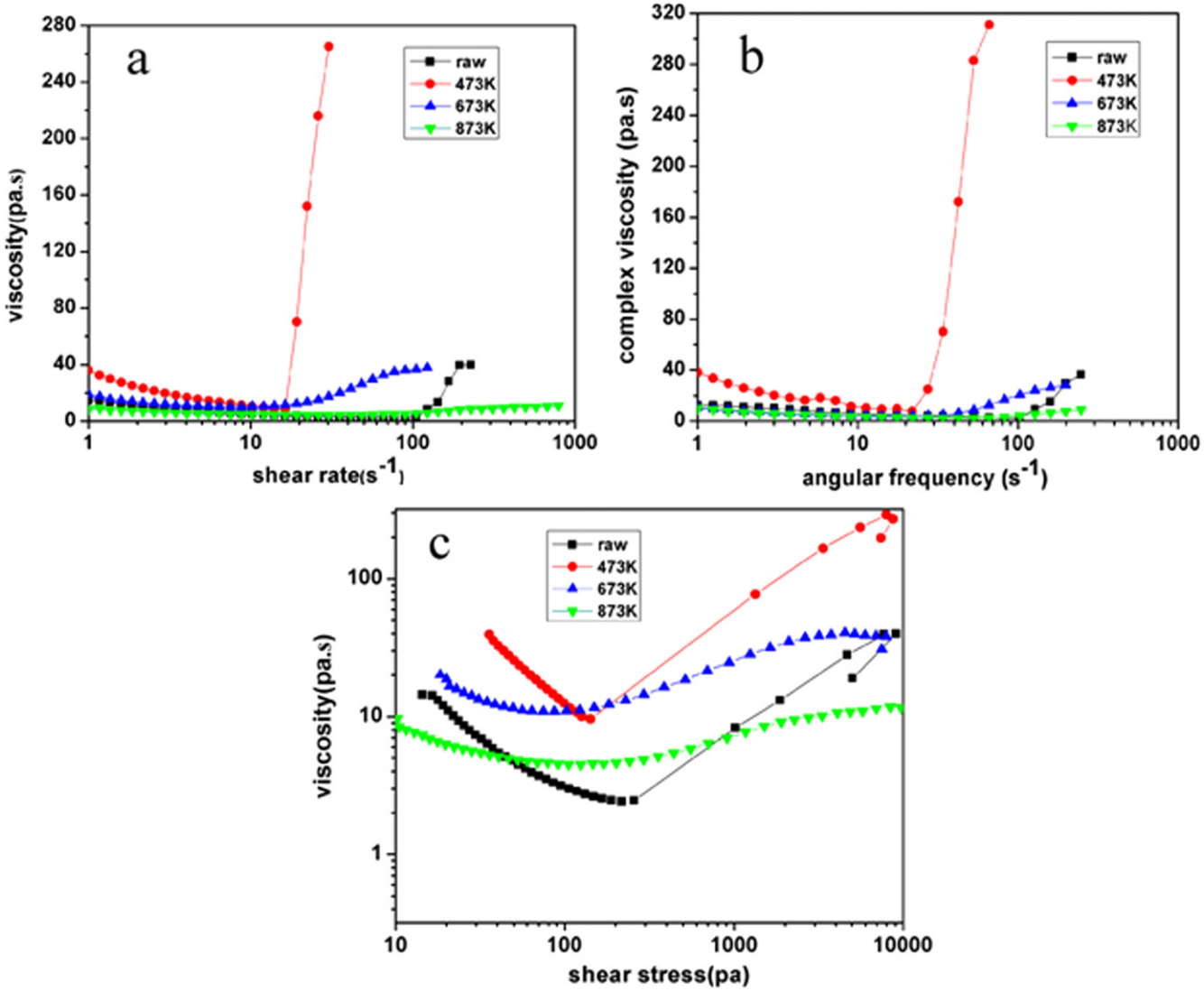

Figure 3. (a) Viscosity versus shear rate for different calcinations temperatures; (b) complex viscosity versus angular frequency for different calcinations temperatures; and (c) viscosity versus shear stress for different calcinations temperatures. The suspension volume fraction was the same 61.2%.

as a reference for other peaks, is from the C element, which resulted from the residual organic ethyoxyl due to the incomplete hydrolyzing TEOS. O 1s and its content change as a function of heating temperature are clearly observed in figure 5(b). The content of oxygen on the silica microspheres surface reached the maximum at 473 K, and then decreased with increasing calcined temperature. The atom ratio of Si to O was found to decrease from 2.2 to 2.0 with increasing heat treatment temperatures (the former ratio being higher than 2 because of the contribution of silanol groups on the surface). These XPS results suggest that the maximum of the silanol groups appears at 473 K. When the calcined temperatures rise higher, the numbers of the silanol groups on the silica microspheres surface become lower. More silanol groups lead to a more adsorped liquid molecule, which further facilitates the thicker solvation layer. Therefore, a high ST effect was obtained.

For given particles and liquid suspension, the critical shear rate is closely related to the volume fraction; the higher volume fraction compresses particles closer and tends to form clusters at low shear rate [22]. Previous results suggested that the critical stress was independent of the volume fraction, but sensitive to particle size and the critical stress decreased with increasing particle size [41, 42]. The magnitude of the ST effect progressively increased with silica volume fraction while at the same time the point of incipient ST was shifted toward lower shear rates [19].

The formation of a solvation layer not only increases the repulsive force but also increases the solid volume fraction by increasing the effective particle size. As the calcined temperature increased from 473 K to 673 K and 873 K, the magnitude of the ST effect decreased, even lower than the raw silica suspension, at the same time the critical shear rate decreases. These results agreed well with previous reports.

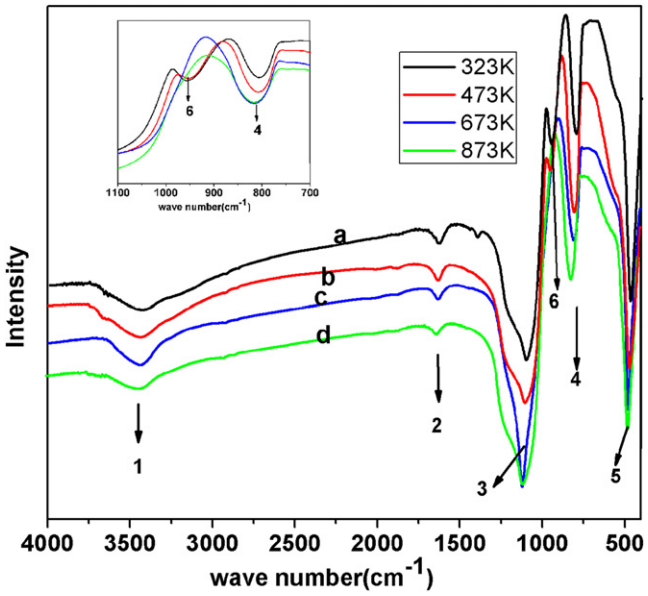

Figure 4. FT-IR spectra of the silica nanoparticles (a)–(d).

The schematic illustration of the effect of silica-calcined treatment via the change of silanol groups on the rheological properties is shown in figure 6. The chemisorption water (silanol groups) on the surface started to condense and evolve water extensively with the increasing calcined temperature, especially the temperature beyond 473 K, which is the threshold temperature for the beginning of dehydroxylation. The infrared absorption of bending vibration at 950 cm^{-1} (paired vicinal silanol groups are shown in table 1) disappeared when the calcined temperature reached over 673 k, as shown in figure 4. It indicated that the silanol groups were removed gradually with the increasing temperature of calcination treatment. The reduction of silanol groups weakened the solvation repulsive force due to the decreased solvation layer. The silanol groups on the silica surface give rise to short-range repulsive forces, and the rate of the surface silanol groups was proportional to the magnitude of the short-range repulsive forces, which resulted in ST. Therefore, under low calcination temperature (473 K), there are enough silanol groups on the surface of the silica to support the ST layer, thus they presented the best ST effects. Once the temperature is too high, not only the adsorped water but also the silanol groups gradually decreased, the hot point for the ST layer decreased, therefore, the ST effects sharply decreased.

Table 1. Peaks of infrared absorption and the function groups of silica particles.

Peak	Wavenumber	Molecular function group
1	3465	molecular H_2O
2	1633	molecular H_2O
3	1100	asymmetric stretching vibration of ≡Si-O-Si≡
4	800	symmetric stretching vibration of ≡Si-O-Si≡
5	470	bending vibration of ≡Si-O-Si≡
6	950	bending vibration of ≡Si-OH

4. Conclusions

This work reported a high performance STF that was prepared by calcinating the dispersing silica microparticles. The influences of the calcination temperature on the rheological properties of the relative STFs were discussed. It was found that the physically adsorbed water and silanol groups on the surface of the silica microspheres were highly dependent on the calcination temperature. The 473 K was proven to be the optimum treating temperature for the STF. A possible mechanism was proposed to analyze the temperature effects and it was found that the surface silanol groups on the silica particles served as the centers for the solvation layer adsorbed on the silica surface. The higher ST degree caused by the

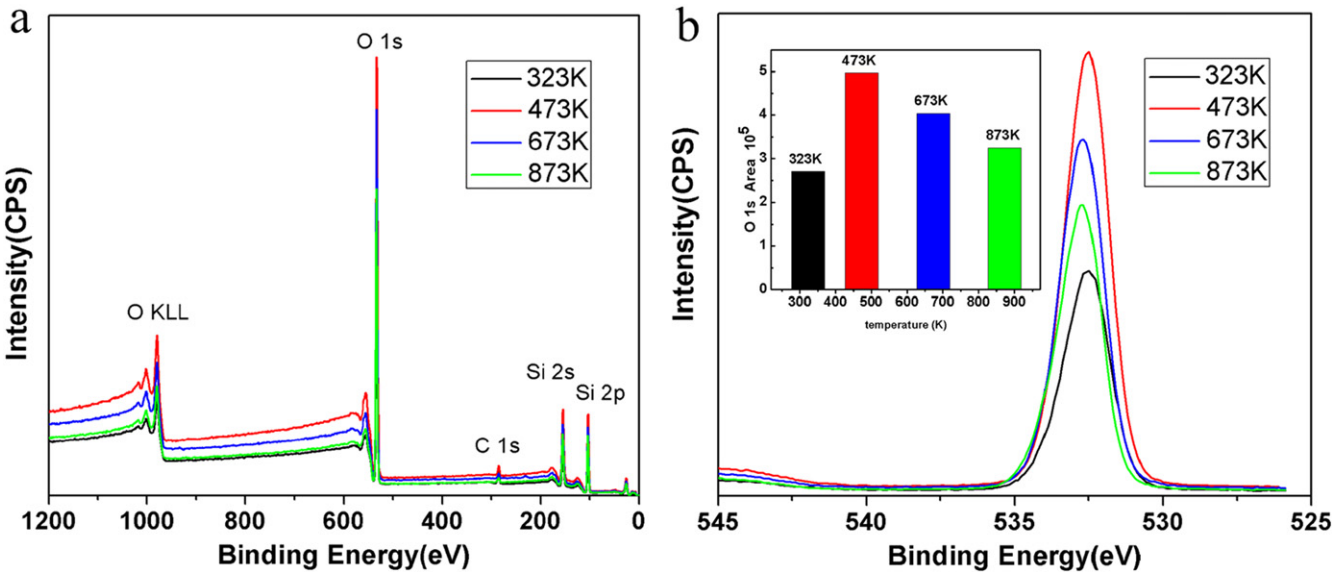

Figure 5. (a) XPS spectra of silica particles for different calcinations temperatures and (b) expanded view of O 1s.

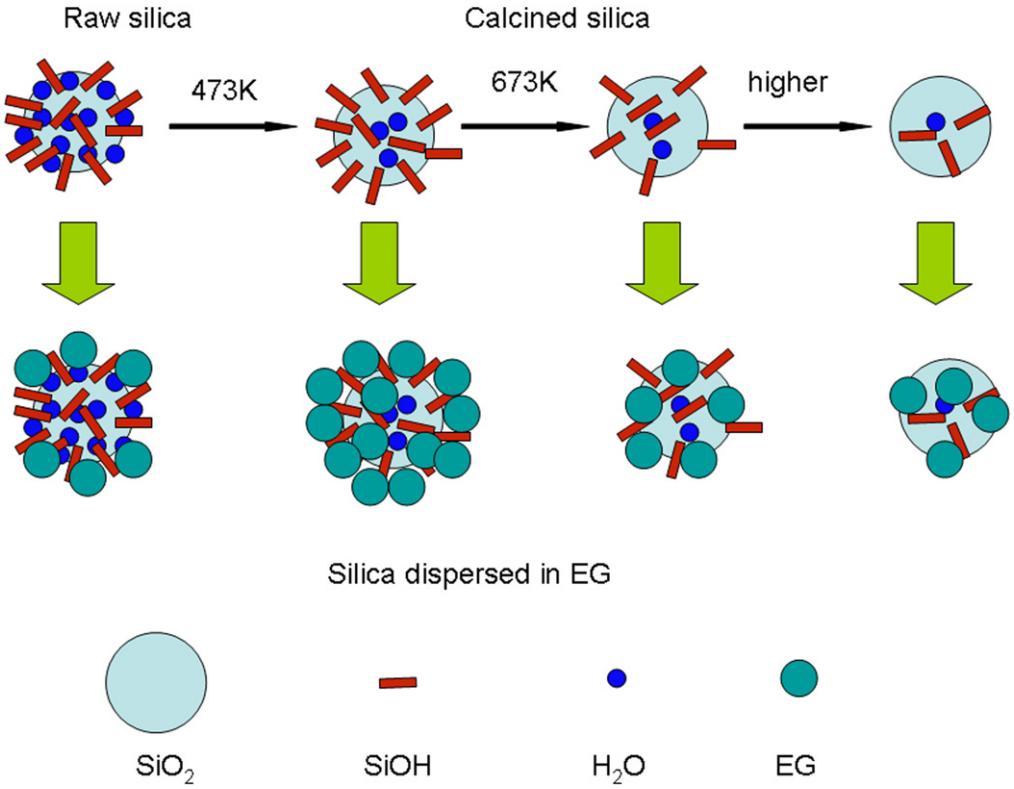

Figure 6. Effect of the calcined temperature on the structure of the silica nanospheres.

solvation layer gave rise to a repulsive interparticle force. This result gives valuable information to further understand the mechanism for the ST effects.

Acknowledgments

Financial support from the National Natural Science Foundation of China (Grant no. 11125210), the National Basic Research Program of China (973 Program, Grant no. 2012CB937500), the Natural Science Foundation of Anhui Province of China (no. KJ2013Z047), and the Anhui Science and Technology University Science Foundation for Youths (no. ZRC2013332) is gratefully acknowledged. This work was supported by the Collaborative Innovation Center of Suzhou Nano Science and Technology.

References

[1] Barnes H A 1989 Shear-thickening (dilatancy) in suspensions of nonaggregating solid particles dispersed in Newtonian liquids *J. Rheol.* **33** 329–66
[2] Boersma W H, Laven J and Pearson D S 1990 Shear thickening (dilatancy) in concentrated dispersions *AIChE J.* **36** 321–32
[3] Brown E and Forman N A 2010 Generality of shear thickening in dense suspensions *Nat. Mater.* **9** 220–4
[4] Lee Y S, Wetzel E D and Wagner N J 2003 The ballistic impact characteristics of Kevlar woven fabrics impregnated with a colloidal shear thickening fluid *J. Mater. Sci.* **38** 2825–33
[5] Xu Y L, Gong X L, Sun Y Q, Xuan S H, Jiang W Q and Zhang Z 2011 Evolution of the initial hole in vertically vibrated shear thickening fluids *Phys. Rev.* E **83** 056311
[6] Zhang X Z, Li W H and Gong X L 2008 The rheology of shear thickening fluid (STF) and the dynamic performance of an STF-filled damper *Smart Mater. Struct.* **17** 035027
[7] Hoffman R L 1972 Discontinuous and dilatant viscosity behavior in concentrated suspensions: 1. Observation of a flow instability *Trans. Soc. Rheol.* **16** 155–73
[8] Hoffman R L 1974 Discontinuous and dilatant viscosity behavior in concentrated suspensions: 2. Theory and experimental tests *J. Colloid Interface Sci.* **46** 491–506
[9] Hoffman R L 1998 Explanations for the cause of shear thickening in concentrated colloidal suspensions *J. Rheol.* **42** 111–23
[10] Bossis G and Brady J F 1989 The rheology of Brownian suspensions *J. Chem. Phys.* **91** 1866–74
[11] Bender J and Wagner N J 1996 Reversible shear thickening in monodisperse and bidisperse colloidal dispersions *J. Rheol.* **40** 899–916
[12] Catherall A A, Melrose J R and Ball R C 2000 Shear thickening and order-disorder effects in concentrated colloids at high shear rates *J. Rheol.* **44** 1–25
[13] Foss D R and Brady J F 2000 Structure, diffusion and rheology of Brownian suspensions by Stokesian dynamics simulation *J. Fluid Mech.* **407** 167–200
[14] Melrose J R 2003 Colloid flow during thickening—a particle level understanding for core–shell particles *Faraday Discuss.* **123** 355–68
[15] Smith W E and Zukoski C F 2004 Flow properties of hard structured particle suspensions *J. Rheol.* **48** 1375–88

[16] Ndong R S and Russel W B 2012 Rheology of surface-modified titania nanoparticles dispersed in PDMS melts: the significance of the power law *J. Rheol.* **56** 27–43
[17] Jiang W Q, Sun Y Q, Xu Y L, Peng C, Gong X L and Zhang Z 2010 Shear-thickening behavior of polymethylmethacrylate particles suspensions in glycerine–water mixtures *Rheol. Acta* **49** 1157–63
[18] Jiang W Q, Ye F, He Q Y, Gong X L, Feng J B, Lu L and Xuan S H 2014 Study of the particles' structure dependent rheological behavior for polymer nanospheres based shear-thickening fluid *J. Colloid Interface Sci.* **413** 8–16
[19] Gopalakrishnan V and Zukoski C F 2004 Effect of attractions on shear thickening in dense suspensions *J. Rheol.* **48** 1321–44
[20] Rueb C J and Zukoski C F 1998 Rheology of suspensions of weakly attractive particles: approach to gelation *J. Rheol.* **42** 1451–76
[21] Raghavan S R, Walls H J and Khan S A 2000 Rheology of silica dispersions in organic liquids: new evidence for solvation forces dictated by hydrogen bonding *Langmuir* **16** 7920–30
[22] Franks G V, Zhou Z W, Duin N J and Boger D V 2000 Effect of interparticle forces on shear thickening of oxide suspensions *J. Rheol.* **44** 759–79
[23] Chu B J, Brady A T, Mannhalter B D and Salem D R 2014 Effect of silica particle surface chemistry on the shear thickening behavior of concentrated colloidal suspensions *J. Phys. D: Appl. Phys.* **47** 335302
[24] Chen Q, Zhu W, Ye F, Gong X L, Jiang W Q and Xuan S H 2014 pH effects on shear thickening behaviors of polystyrene-ethylacrylate colloidal dispersions *Mater. Res. Exp.* **1** 015303
[25] Chen Q, Zhu W, Ye F, Gong X L, Jiang W Q and Xuan S H 2014 pH effects on shear thickening behaviors of polystyrene-ethylacrylate colloidal dispersions *Mater. Res. Exp.* **1** 015303
[26] Ye F, Zhu W, Jiang W Q, Wang Z Y, Chen Q, Gong X L and Xuan S H 2013 Influence of surfactants on shear thickening behavior in concentrated polymer dispersions *J. Nanopart. Res.* **15** 2122
[27] Franks G V 2002 Zeta potentials and yield stresses of silica suspensions in concentrated monovalent electrolytes: isoelectric point shift and additional attraction *J. Colloid Interface Sci.* **249** 44–51
[28] Fagan M E and Zukoski C F 1997 The rheology of charge stabilized suspensions *J. Rheol.* **44** 373–97
[29] Heine D R, Petersen M K and Grest G S 2010 Effect of particle shape and charge on bulk rheology of nanoparticle suspensions *J. Chem. Phys.* **132** 184509
[30] Shenoy S S and Wagner N J 2005 Influence of medium viscosity and adsorbed polymer on the reversible shear thickening transition in concentrated colloidal dispersions *Rheol. Acta* **44** 360–71
[31] Xu Y L, Gong X L, Peng C, Sun Y Q, Jiang W Q and Zhang Z 2010 Shear thickening fluids based on additives with different concentrations and molecular chain lengths *Chin. J. Chem. Phys.* **23** 342–6
[32] Kaldasch J, Senge B and Laven J 2008 Shear thickening in electrically stabilized colloidal suspensions *Rheol. Acta* **47** 319–23
[33] Kaldasch J, Senge B and Laven J 2009 The impact of non-DLVO forces on the onset of shear thickening of concentrated electrically stabilized suspensions *Rheol. Acta* **48** 665–72
[34] Liu P, Wang Q S, Li X and Zhang C C 2009 Investigation of the states of water and OH groups on the surface of silica *Colloids Surf.* A **334** 112–5
[35] Zharavlev L T 1993 Surface characterization of amorphous silica—a review of work from the former USSR *Colloids Surf.* A **74** 71–90
[36] Zharavlev L T 2000 The surface chemistry of amorphous silica. Zhuravlev model *Colloids Surf.* A **173** 1–38
[37] Zharavlev L T 2006 *Colloddal silica: Fundamentals and Applications* ed H E Bergna and W O Roberts (Boca Raton: CRC Press) pp 261–6
[38] Stöber W, Fink A and Bohn E 1968 Controlled growth of monodisperse silica spheres in micron size range *J. Colloid Interface Sci.* **26** 62–9
[39] Yin J B, Wang X X and Zhao X P 2015 Silicone-grafted carbonaceous nanotubes with enhanced dispersion stability and electrorheological efficiency *Nanotechnology* **26** 065704
[40] Shallenberger J R 1996 Determination of chemistry and microstructure in SiOx ($0.1 < x < 0.8$) films by x-ray photoelectron spectroscopy *J. Vac. Sci. Technol.* A **14** 693–8
[41] Maranzano B J and Wagner N J 2001 The effects of interparticle interactions and particle size on reversible shear thickening: hard-sphere colloidal dispersions *J. Rheol.* **45** 1205–22
[42] Maranzano B J and Wagner N J 2001 The effects of particle size on reversible shear thickening of concentrated colloidal dispersions *J. Chem. Phys.* **114** 10514–27